

# Deposition of Aerosol Particles in Fibrous Filters

D. G. THOMAS and C. E. LAPPLE

The Ohio State University, Columbus, Ohio

The collection efficiency of glass fiber pads was investigated with a super cooled liquid aerosol. A filter-velocity range of 0.02 to 20 ft./sec. was covered with filter pads having a bulk density ranging from 1 to 10 lb./cu. ft. and a fiber diameter ranging from 1 to 30  $\mu$ .

For the aerosol employed the results showed a minimum collection efficiency at a velocity of 2 to 5 ft./sec., dependent on fiber size. At the lower velocities, where diffusion is controlling, collection efficiency increased with decreased velocity; at higher velocities, where inertia is controlling, efficiency increased with increased velocity.

For purposes of generalization the data were correlated in terms of dimensionless parameters which allow for the combined effects of flow-line interception, inertial interception, and diffusional deposition. Evaluation of the data in terms of existing theories of deposition indicated nominal agreement with the theory of Langmuir, as modified by Natanson, for diffusional deposition. For inertial deposition the measured collection efficiencies were considerably lower than would be predicted from the theoretical values reported by Langmuir and Blodgett for potential flow around the fibers, presumably because of the viscous-flow (low Reynolds number) conditions that prevailed in this study.

Filters consisting of a packing of fibrous or granular material have been widely used for removing aerosol particles from a gas stream. Typical applications are domestic furnace air filters, coke beds for removal of sulfuric acid mist, and sand, glass, or asbestos fiber filters for exhaust gases which contain radioactive or biologically active particles.

The fundamental mechanisms of deposition of aerosol particles on single bodies or collections of bodies (or in filters) have been considered both experimentally and theoretically by a number of investigators (1 to 17). However these investigations usually have been restricted to simplified or narrow ranges of conditions, and experimental data are relatively meager.

The present study was undertaken to obtain experimental data on the collection of aerosol particles in fibrous filters over a sufficiently wide range of conditions to provide a basis for arriving at a generalized means for pre-

dicting deposition in fibrous filter media. This study was restricted to clean fibrous media, in which insufficient aerosol particles had been deposited for the deposit itself to influence significantly the deposition mechanism.

## BASIC CONCEPTS

### Collection Efficiency

The efficiency of a filter is commonly expressed as the weight fraction of aerosol collected by the filter. Often the fraction passing the filter is of primary interest. Since this fraction is usually exponentially related to the properties of the pad, it is more convenient to express efficiency in terms of the transfer unit defined by

$$N_t = \ln [1/(1 - \eta_t)] \quad (1)$$

or

$$\eta_t = 1 - e^{-N_t} \quad (1a)$$

Table 1 gives corresponding values of  $N_t$  and  $\eta_t$  calculated from Equation (1) in order to provide a numerical conception of the relationship.

$N_t$  is a direct measure of the effectiveness of the filtration. It is analogous to the similar term used in mass transfer (absorption, distillation) problems where there is negligible back pressure above the absorbing phase. (Negligible back pressure is comparable with the absence of re-entrainment of aerosol particles once they have been deposited.) Also  $N_t$  is directly related to the decontamination factor which has been widely used in automatic energy filtration applications (1):

$$N_t = 2.303 (D.F.) \quad (2)$$

The terms  $\eta_t$ ,  $N_t$ , and  $D.F.$  are measures of the over-all collection efficiency of complete filter pads or filters. With homogeneous aerosols the number of transfer units for pads in series (that is the over-all transfer units) is equal to the sum of the number of transfer units for each individual pad.

### Target Efficiency

Instead of expressing efficiency of a gross pad it is desirable for purposes of generalization to relate collection efficiency to the individual fibers in the pad to remove from consideration, insofar as possible, the specific details of pad construction (depth and den-

D. G. Thomas is with Oak Ridge National Laboratory, Oak Ridge, Tennessee; C. E. Lapple is with Stanford Research Institute, Menlo Park, California.

sity). It has been customary to express deposition on individual body surfaces, such as cylinders or spheres, in terms of a target efficiency. Target efficiency is defined as the ratio of aerosol material collected on the body to the total aerosol material contained in the gas stream swept out by the body.

For the case where cylindrical fibers are normal to the direction of gas flow it is readily shown that target efficiency is related to transfer units for the whole pad by

$$\eta_t = (\pi D_b N_t / 4) / (m_t / \rho_b A_f) \\ = (\pi D_b N_t) / [4 L_f (1 - \epsilon_v)] \quad (3)^*$$

In the derivation of Equation (3) it is assumed that (1)  $\eta_t$  is constant throughout the filter, (2) the fractional deposition in any one layer of fiber is relatively small, and (3) in successive layers of fiber there is essentially complete remixing of the gas before any large fraction of aerosol approaching any of these layers has been deposited. The first assumption restricts Equation (3) to homogeneous aerosols. In heterogeneous aerosols however Equation (3) will still express the performance characteristics for any given particle size if it is recognized that the terms  $N_t$  and  $\eta_t$  in Equation (1) will then represent the performance for that same size. Assumptions (2) and (3) are generally good approximations for filters which consist of a large number of fiber layers. This has been demonstrated by the fact that successive identical pads in series give the same values of  $N_t$  or  $\eta_t$  with homogeneous aerosols. Where the fibers are not cylindrical or not normal to the direction of gas flow, an additional proportionality factor must be provided in Equation (3).

For the purposes of subsequent correlations of data Equation (3) may be regarded as a definition of  $\eta_t$  without affecting the validity of the correlations. The distinction between  $\eta_t$  as a defined term and as a derived term would only enter into a comparison of data correlations with theoretical predictions derived for deposition on individual fibers.

#### Deposition Mechanisms

As discussed in more detail by Lunde and Lapple (9) the magnitude of the target efficiency is dependent on the nature of the mechanism by which the aerosol particles are deposited on the fiber. There are six such mechanisms: flow-line (or direct) interception, inertial interception, grav-

ity settling, diffusional migration, electrostatic migration, and thermal migration. The magnitude of each of the mechanisms is measurable in terms of a specific dimensionless parameter  $N_i$ , which may be termed a "separation number." In other words target efficiency is a function of each of these parameters in addition to any other parameters, such as Reynolds number or pad density, which measure the relative effects of changes in flow pattern.

By dimensional analysis it may be shown that for the general case  $\eta_t$  is a function of some two dozen dimensionless groups, which include all of the  $N_i$  terms in addition to other groups which measure modifying influences on the flow pattern and force fields (9). For purposes of simplification it may be assumed (1) that the gravitational, electrostatic, and thermal depositions are negligible; (2) that compressibility effects are negligible; and (3) that slip or molecular flow effects may be neglected except insofar as they are incorporated by the Stokes-Cunningham correction factor. Justification for these assumptions is based on the following arguments: (1) Relative to other deposition mechanisms gravitational settling would normally be expected to be significant only with aerosol particles larger than approximately  $1 \mu$  in diameter and with collecting bodies larger than some  $100 \mu$  in diameter when operated at low filter velocities. Gravity settling would be expected to act somewhat independently of the other mechanisms with little interactive effect. Consequently for most purposes gravity settling may be treated as a separate additive effect on target efficiency, having a magnitude numerically equivalent to the order of the value of  $N_{sg}$ . Thermal deposition will be negligible if no marked temperature gradients exist. Possible electrostatic effects will be discussed later. (2) The absence of

compressibility effects requires that pressure drop across the filter be small compared with the absolute pressure. (3) The absence of slip- or molecular-flow effects requires that the mean-free path of the gas molecules be small compared with the filter fiber diameter. The Stokes-Cunningham correction factor represents a means of allowing for slip-flow effects around the aerosol particles.

With the above simplifications it can be shown from dimensional analysis that a unique functional relationship must exist between  $\eta_t$  and the various parameters as indicated by the following specific alternative equations:

$$\eta_t = \psi_1 [N_{st}, N_{si}, N_{sd}, N_{Re}, \epsilon_v] \quad (4)$$

$$\eta_t = \psi_2 [N_{st}, N_{si}, N_{sc}, N_{Re}, \epsilon_v] \quad (4a)$$

$$\eta_t = \psi_3 [N_{st}, N_{sd}, N_{sc}, N_{Re}, \epsilon_v] \quad (4b)$$

$$\eta_t = \psi_4 [N_{st}, N_{si}, N_{sc}, N_p, \epsilon_v] \quad (4c)$$

$$\eta_t = \psi_5 [N_{st}, N_{sd}, N_{sc}, N_p, \epsilon_v] \quad (4d)$$

The term  $N_{sc}$  is analogous to the Schmidt number in mass transfer and contains a measure of the interactive effect of flow line and inertial interception and diffusional deposition. The term  $N_p$  allows for additional flow-pattern effects not already incorporated through the terms  $N_{st}$  and  $N_{si}$ , both of which incorporate a measure of some Reynolds number effects in addition to measuring their respective deposition mechanisms. This follows from the fact that  $N_p$  is mathematically equivalent to  $N_{st}/N_{Re} N_{si}$ . The Schmidt number is actually the reciprocal of the product of  $N_{sc}$  and  $N_p$  and could be used as an alternative to either of these groups in a relationship of the type indicated in Equations (4).

As stated, Equations (4) apply only to geometrically similar fibrous packings. In order to generalize to any geometry additional terms are required to allow for variations in packing geometry, such as fiber shape, relative fiber spacing and orientation, and relative fiber size distribution. In the subsequent discussion these additional factors are ignored as variables. The effect of variations in these factors, which were not all controlled separately in this study, is believed to be of secondary importance for the range of conditions employed. Glass fibers, used in this study, are universally circular in cross section and, as normally available, will involve a preponderance of fibers oriented normal to one direction (the direction of gas flow in this study). A variation in  $\epsilon_v$  due to compressing such a packing would be expected to reflect primarily as a variation in longitudinal fiber spacing

TABLE I. RELATIONSHIP BETWEEN  
COLLECTION EFFICIENCY AND  
TRANSFER UNITS

Number of transfer units, $N_t$	Collection efficiency $\eta_t$ , %
0.1*	9.5
0.5	39.4
1	63.2
2	86.47
3	95.02
4	98.17
6	99.75
10	99.9955

\* For values of  $N_t$  less than 0.1 the collection efficiency  $\eta_t$  expressed as a fraction, essentially is numerically identical to  $N_{st}$ .

\* A derivation given by Chen (2) results in a similar equation with the exception that Chen obtains an additional term  $\epsilon_v$  in the numerator of the right-hand term. This reflects a difference in the definition of  $\eta_t$  which is strictly arbitrary when dealing with proximate fibers.

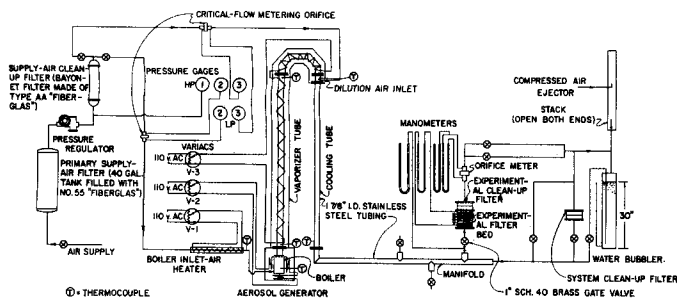


Fig. 1. Schematic diagram of equipment.

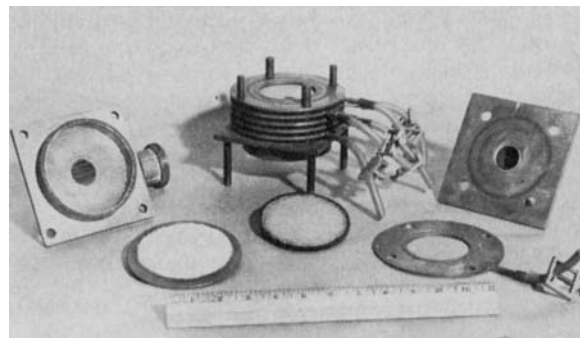


Fig. 2. Photograph of disassembled test filter assembly.

with relatively little change in lateral fiber spacing.

It should be noted that both  $N_{t,0}$  and  $N_p$  involve only the properties of the aerosol particles and of the fluid; they do not involve filtration velocity or filter-pad properties. Thus for a given aerosol and fluid, and subject to the limitations made in deriving Equations (4), a unique relationship is to be expected between  $\eta_t$  and  $N_{t,0}$ ,  $N_{t,0}$  and  $\epsilon_t$ , or between  $\eta_t$  and  $N_{t,0}$ ,  $N_{t,0}$  and  $\epsilon_t$ , regardless of variations in operating conditions and filter pad properties.

If the functional relationship implied by Equations (4) is known, either analytically or experimentally, the target efficiency can be calculated for any fiber configuration, operating condition, and aerosol. From target efficiency, transfer units and collection efficiency can be calculated directly from Equations (3) and (1), respectively.

Several investigators have attempted to develop analytically the relationship of Equation (4) for conditions where only one or the other of the separating mechanisms is controlling. To date however no general solution has been developed. It was the purpose of the current investigation to develop this relationship experimentally.

## EXPERIMENTAL EQUIPMENT AND PROCEDURE

In the experimental investigation a test aerosol was passed through individual pads of glass fiber mats in series. Collection efficiencies were measured over a wide range of air velocities by determining the amount of aerosol retained in each pad and the amount that passed the series of pads. Figure 1 presents a schematic diagram of the apparatus used.

In order to take advantage of the convenience of colorimetric analytical techniques a volatile dye was used. The test aerosol was prepared by bubbling hot filtered air through a pool of molten dye in a large-scale, stainless-steel version of the Sinclair-La Mer generator. The air and dye vapors, after passing through a superheater, were quenched suddenly with filtered room-temperature air to form the aerosol. No nucleation was employed. Throughout all the tests the generator con-

ditions were held constant to give a constant reproducible aerosol as determined by frequent checks of filtration efficiency on a given filter pad arrangement. The size of the aerosol particles was determined with a single-stage jet impactor borrowed from the University of Illinois (13). The jet was rectangular with slot dimensions approximately 0.05 cm. by 1 cm. From 0.02 to 3 mg. of dye was collected in the jet collector cup, representing approximately 1 to 60% of the total dye entering the jet impactor, respectively.

The filter pads were made by mounting weighed amounts of glass fiber between permanent 16-mesh copper screens soldered to a 0.108 in. thick spacer ring. All test fibers were fired at 400°C. to remove any binder or lubricant. Five pads were mounted in series in each test and were followed by a cleanup filter consisting of two mats in series. Figure 2 shows the disassembled filter unit with four experimental pads and spacers in place. The fifth pad, the cleanup filter, and the two end plates are shown in front of the assembly together with a typical brass-spacer plate used between each pad for pressure drop measurements.

The aerosol generator was operated for at least 3 hr. prior to making efficiency

determinations. After steady state was attained, as determined by thermocouple readings, the aerosol was passed through the experimental filter bed and cleanup filter. The pressure drop was checked near the start and at the end of the run; no significant increase in pressure drop was observed during any runs. Flow rates were measured with critical flow meters or orifices. At the conclusion of the test the filter bed was disassembled, the dye leached from each test filter and from the cleanup filter with benzene, and the dye solution analyzed colorimetrically. A summary of the range of experimental conditions covered in the investigation is given in Table 2.

## EXPERIMENTAL RESULTS

Data from typical runs are presented in Figure 3. The variations shown for successive pads in runs 17, 20, and 117 are typical of most of the data, with measured collection efficiencies expressed as transfer units for successive pads varying by approximately  $\pm 20\%$  from the average. The average of the values measured for each pad was used for subsequent correlations. Run 37 represents an occasional run in which wider variations in successive pads were obtained. Occasionally data such as shown for run 38 were obtained, where the first pad showed a very high efficiency whereas the subsequent pads were in agreement. This was usually encountered with high velocities (16 ft./sec. filter velocity in the case of run 38) and was attributed to flocs of aerosol particles dislodged from a small accumulation on the ductwork following the aerosol generator. Data from such runs were discarded and the run repeated. Run 94 is typical of substantially all runs in which the collection efficiency was greater than one transfer unit (63% collection) for the first pad. In these runs each successive pad showed a lower collection efficiency. This was attributed to the fact that the aerosol was not entirely homogeneous in size, the first pad removing the size most readily deposited and successive pads being exposed progressively to those aerosol particles more difficult to de-

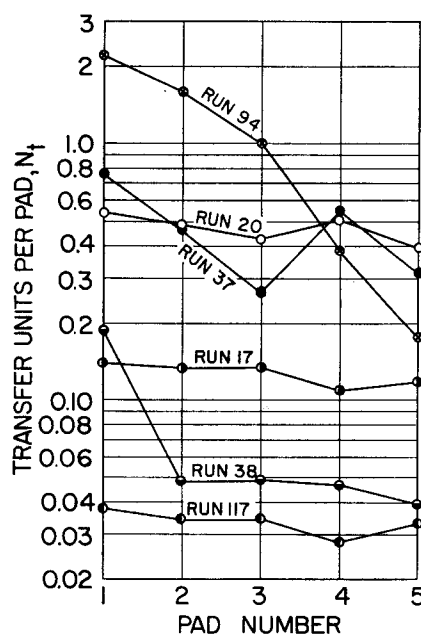


Fig. 3. Collection efficiency data from typical runs.

posit. Such an effect is actually present in all runs but would be expected to become significant only when relatively large fractions of aerosol particles are removed. Runs similar to run 94 were restricted almost entirely to the pads with F-1 fibers. In these cases the amount collected on the cleanup filter is also very small; thus, the measured collection efficiencies for the later pads in the series are very sensitive to errors in measuring the deposit on the cleanup filter, especially slight contamination thereof. Consequently for all such runs the collection efficiency measured for the first pad was chosen for subsequent correlations as most representative of performance with the specific feed aerosol.

The data for all runs are summarized in Figure 4 as a plot of transfer unit per pad against superficial filter velocity for the various fiber sizes and pad densities. Each point represents the average measured efficiency for five pads in series or for the first pad as discussed above. The curves for all fibers and densities have a similar shape. At high velocity inertial interception is the controlling mechanism; as the velocity is reduced, inertial interception becomes less effective and collection efficiency decreases. At low velocities diffusion becomes the controlling deposition mechanism and collection efficiency increases with further decrease in velocity. The flattening of the curves for the fine fibers may be attributed to the superimposed effect of flow-line interception, which is relatively more pronounced with the fine fibers, whose magnitude is relatively independent of gas velocity. All the data from a series of special tests, described below, are also incorporated in Figure 4.

Special tests were made with the filter pads oriented so that the flow was either vertically upward or vertically downward as compared with the usual horizontal flow. These tests were made with pads made of F-1, F-3, and F-4 fiber at velocities ranging from 0.02 to 2 ft./sec. Within the precision of the data no effect of this orientation on collection efficiency was observed, indicating a negligible effect of the gravitational deposition mechanism.

In another series of special tests the fibers were coated with 10% by weight of mineral oil, in which the aerosol dye particles are soluble, in an attempt to determine if aerosol particles striking a fiber will adhere. These tests were made with pads of F-1 and F-3 fiber at a velocity of 1 ft./sec. Within the general precision no effect of this coating on collection efficiency was observed. These results would indicate,

although not conclusively, that all aerosol particles striking a fiber adhered. These results would also support the belief that those electrostatic deposition effects, which would be expected to depend on the surface characteristics of the fiber, were not important in these tests.

### CORRELATION OF DATA

Although the data are presented directly in Figure 4, for purposes of generalization it is necessary to evaluate them in terms of fundamental concepts. This may be done by using the data as a means for evaluating the nature of the functional relationship implied by Equations (4).

In order to convert the data of Figure 4 into the form required by Equations (4) it is necessary to make use of the aerosol and fiber properties, given in Table 2. As discussed in detail in the Appendix it was inferred from work subsequent to that reported here that the aerosol particle diameter was actually  $0.29 \mu$  rather than the  $0.40 \mu$  originally measured and that the specific surface average diameter of fiber F-1 was  $2.3 \mu$  rather than the  $1.29 \mu$  originally reported. Since the time lapse between the investigation made it physically impossible to check these implied corrections experimentally, these corrections must be considered as a possible limitation on the absolute accuracy of the correlations. It is for this reason that the correlation will be presented on both an uncorrected and a corrected basis in the subsequent discussion.

It is believed that the corrected aerosol size is reasonably valid. The correction on the diameter of fiber F-1 is probably in the right direction but is quantitatively more questionable. The quantitative magnitude of these corrections on each of the correlation parameters is indicated in the Appendix. While these corrections are quite

significant, it should be noted that because of limitations in current techniques of size measurement unknown absolute errors of this magnitude may be present in many of the data of this type reported in the literature.

Since the gas and the aerosol properties were both held constant throughout this study, the value of both parameters  $N_{sc}$  and  $N_s$  remained constant (2140 and 80, respectively, on the uncorrected basis; 1270 and 89, corrected basis). Thus as previously discussed a unique correlation is to be expected when target efficiency is plotted against either the inertial interception parameter  $N_{si}$  or the diffusional separation parameter  $N_{sd}$ , with  $N_{si}$  and  $\epsilon_v$  as parameters. To test this conclusion the experimental data shown in Figure 4 have been converted to the forms shown in Figures 5 and 6 on both an uncorrected and a corrected basis. It should be emphasized that Figures 5 and 6 are not independent; they are merely alternate, mathematically identical ways of presenting the data. Since the interaction parameter  $N_{se}$  is constant, once any two of the three separation numbers  $N_{si}$ ,  $N_{sd}$ , and  $N_{se}$  are fixed, the third is determined. The value of the third parameter, corresponding to the solid lines used to represent the data, is shown as a dashed line in each figure. Figures 5 and 6 may be regarded as the graphical manifestation of the functional relationships implied by Equations (4c) and (4d), respectively, for the specific values of  $N_{sc}$  and  $N_s$ .

Equations (4c) and (4d) imply that target efficiency may be a function of pad porosity  $\epsilon_v$  as well as of the other parameters. Hydrodynamic considerations (6) lead to the expectation that increased bed density (reduced porosity) should result in increased target efficiency, other factors remaining constant. In Figures 5 and 6 bed-density variations for a given fiber (and correspondingly for a given  $N_{si}$ ) are indicated by the degree of shading of the data points. In general the data for a given fiber show no distinct effect of bed density on target efficiency, within the precision of the data, although there appears to be an indication of a trend toward higher efficiencies with increased bed density in the case of the fiber F-1 pads. Since the bed densities were not varied too widely however, it can only be concluded that the effect of bed density (or porosity) on target efficiency is minor, at least over the range of densities investigated. It is for this reason that single solid lines have been drawn through all the data for a given fiber, regardless of the bed density involved.

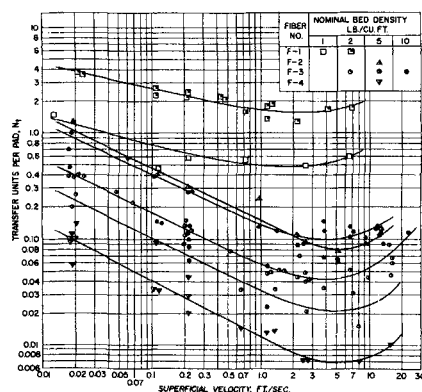


Fig. 4. Summary of experimental collection efficiency data.

TABLE 2. SUMMARY OF RANGE OF EXPERIMENTAL CONDITIONS

## Filter pads:

Type fiber:	Glass (sp. gr. = 2.50)			Geometric std. deviation
Fiber sizes:	Fiber no.	Trade name (Owens-Corning Fiberglas Corp.)	Average fiber diameter*, $\mu$	
	F-1	Aerocor-PF (Type AA)	1.29 (2.3)†	2.4
	F-2	Basic 28	7.6	1.2
	F-3	Fine wool	10.7	1.4
	F-4	Curly wool (Type 115K)	29.4	1.1
Pad densities:	1 to 10 lb./cu. ft.			
Pad thickness:	0.1 in.			
Pad diameter:	1 or $2\frac{1}{2}$ in. (diameter exposed to air flow)			
No. of pads in series:	5			

## Aerosol:

Material:	DuPont oil orange (benzene azo $\beta$ -naphthol), sp. gr. = 1.26, m.p. = 262°F.)
Particle size:	mass median diameter = $0.4\mu$ ( $0.29\mu$ )†, geometric std. deviation = 1.4
Particle character:	supercooled spherical drops, crystallized into needles on shock or after 10 to 20 min.
Gas:	Air at nominally atmospheric pressure and temperature (actually 6 cm. Hg gauge, 27°C.)
Concentration:	1 to 2 mg./cu. ft.
Operating conditions:	

Superficial filter velocity: 0.02 to 20 ft./sec.

\* Specific surface average fiber diameter.

† Value in parenthesis is corrected value as based on later work; see appendix for detail.

From the fact that a correlation was obtained by neglecting electrostatic effects one might conclude that such effects were absent in these tests. If however an electrostatic separation criterion followed the same trend in all the tests as one of the other separation numbers, this conclusion would not be valid. A consideration of the various electrostatic separation criteria (9) reveals that the parameter that measures electrostatic deposition by induction would be directly proportional to the diffusional separation number  $N_{s,d}$  if any surface charge concentration had been the same on all fibers tested. While this would represent a coincidental condition, it is not an unlikely one. The only direct evidence against this possibility is the fact that, as will be shown later, target efficiencies obtained are of the order of magnitude that would be expected if diffusion were a controlling factor in the absence of inductive electrostatic deposition.

## DISCUSSION OF RESULTS

The data of Figures 5 and 6 suggest limiting curves for  $N_{s,r} = 0$ . These

have been drawn in as dotted or short-dashed curves. In Figure 5 this limiting curve may be regarded as the target efficiency at low Reynolds numbers if inertial interception were the only deposition mechanism. In Figure 6 the limiting curve would correspond to the target efficiency to be expected at low Reynolds numbers if diffusion were the only deposition mechanism.

Langmuir (6) reports a calculated value of  $N_{s,r}$  of 0.27 below which no deposition by inertial interception can occur at low Reynolds number in the absence of flow-line interception ( $N_{s,r} = 0$ ) or diffusion ( $N_{s,d} = 0$ ), although he gives no details as to the method of arriving at this value. This value was used as an asymptote in drawing the limiting curve for  $N_{s,r} = 0$  in Figure 5. Also shown as a dotted curve in Figure 5 are the calculated values reported by Langmuir and Blodgett (7) for potential flow. These values would correspond to the target efficiencies to be expected for pure inertial interception (that is for  $N_{s,r}$  and  $N_{s,d} = 0$ ) at very high Reynolds number and should be much greater than those for viscous flow.

Davies (3), Langmuir (6), Lewis and Smith (8), Natanson (11), Ranz (12), and Stairmand (16) have all developed analytical expressions for target efficiencies under conditions of pure diffusion to single cylinders. Most of these expressions incorporate a variety of assumptions or approximations and differ from each other by several-fold factors. For negligible flow-line interception ( $N_{s,r} = 0$ ) these relationships may all be expressed in the form

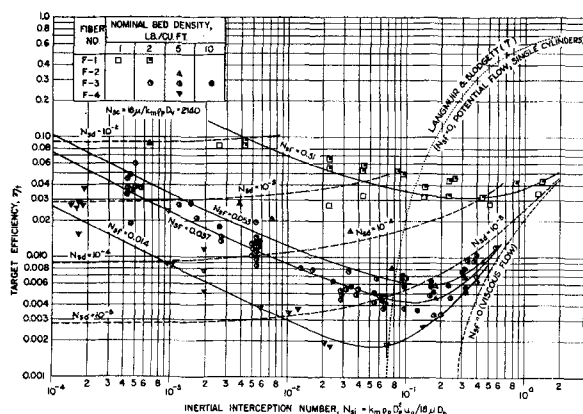
$$\eta_t = a N_{s,d}^n \quad (5)$$

The dotted line in Figure 6 also has this form with  $n = \frac{1}{2}$  and  $a = 0.71$  and 0.87, on the corrected and uncorrected bases, respectively.

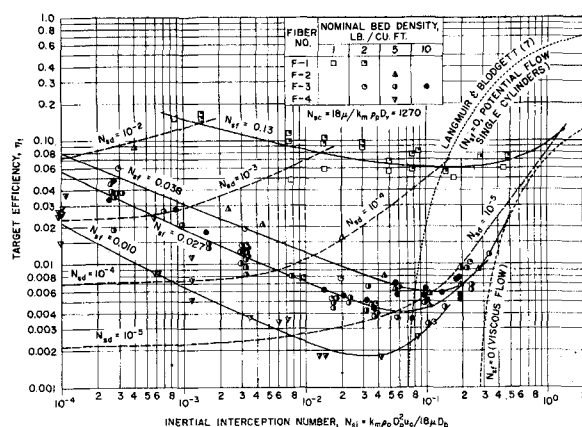
Lewis and Smith, and Stairmand, on the basis of radically simplifying assumptions, obtained a slope  $n$  of  $\frac{1}{2}$ . However their constants  $a$  were  $(\pi k_s/2)$  and  $\sqrt{8}$ , respectively. With the exception of Lewis and Smith all the other investigators have assumed that the sticking factor  $k_s$  is unity. Langmuir's derivation was based on a more detailed consideration of the underlying hydrodynamics. He obtained  $n = 2/3$  and found a minor variation of the value  $a$  with Reynolds number. Ranz's relationships were derived by analogy with the Froessling mass transfer equations and give numerical results closely approximating those of Langmuir. Natanson (11), from a rigorous application of hydrodynamics, obtained equations of the same form as Langmuir but concluded that the target efficiency was 1.71 times that predicted from Langmuir's equations. Davies' (3) equations were based on gross assumptions and led to a value of  $n = 1$ . Numerically, target efficiencies predicted from Davies' equations for the conditions under consideration are considerably lower than those calculated from the relationships of Langmuir and of Ranz.

The experimental conditions in the present tests were such that high values of  $N_{s,d}$  were inherently accompanied by low values of the Reynolds number and vice versa. Thus when appropriate Reynolds numbers are used in making the comparison with either the Langmuir, the Natanson, or the Ranz equations, the net numerical result is approximately the same as though the value of  $a$  in Equation (5) were held constant and  $n$  were reduced to an approximate value of  $\frac{1}{2}$ . In general the target efficiencies indicated by the dotted line of Figure 6 are approximately three times as large as predicted by either the Langmuir or the Ranz equations and approximately two times those predicted from Natanson's equation.

It should be noted that the theoretical equations of Langmuir, Ranz,



a. Uncorrected (based on original data).



b. Corrected (as discussed in Appendix).

Fig. 5. Target efficiency as a function of the inertial separation number.

and Natanson all apply to deposition on completely unbounded cylinders. For this case hydrodynamic considerations show that the value of  $a$  in Equation (5) must decrease continuously as the Reynolds number decreases. For finite or bounded cylinders, such as are encountered in actual filters, it is to be expected that not only will the value of  $a$  be greater than for unbounded cylinders, but it will decrease with decreasing Reynolds number to a certain point. Below a certain Reynolds number however it should remain constant. From considerations involving pressure drop (beyond the scope of this paper) it was concluded that this lower Reynolds number limit decreases as pad porosity increases; however the value of  $a$  should be constant at all Reynolds numbers less than 0.1 for porosity levels encountered in practice. In Figure 6 in place of the dotted curve shown for  $N_{st} = 0$  it would not be unreasonable to assign an alternative limiting line of slope  $n = 2/3$  as representative of low Reynolds numbers, in keeping with the Langmuir and Natanson predictions. Such a line would have a value of  $a$  in the range of 2 to 3. However a rigorous hydrodynamic consideration of bounded cylinders might call for a different value of  $n$  as well. Consequently this question must be considered as unresolved at this time. Experiments aimed at such a resolution require the use of either smaller aerosol particles or lower filtration velocities than were used in this study.

As previously mentioned it is believed that the corrected values in Figures 5 and 6 are of greater absolute accuracy than the uncorrected ones. That is especially true of the data for fibers F-2, F-3, and F-4, which reflect only corrections on aerosol particle size. In fiber F-1 an additional more questionable correction for fiber size is also involved. Since fiber

F-1 involves a relatively heterogeneous fiber as well (uniform fibers of this fine size are not commercially available), the uncertainties arising from defining a proper average fiber size to employ in the correlation may overshadow the magnitude of the correction applied in this case. The specific surface average fiber diameter employed was strictly arbitrary. It is probably a realistic average to use in calculating target efficiency. In the various separation parameters however a different average diameter may be required. It is also likely that this average diameter should be defined differently dependent on the nature of the predominant separation mechanism. This uncertainty is not involved in the case of fibers F-2, F-3, and F-4, all of which were relatively uniform. Thus while the corrected correlations for fibers F-2, 3, and 4 are probably reasonably accurate on an absolute basis, the correlations for fiber F-1 are subject to considerable question as to their absolute (as distinguished from relative) accuracy.

## APPLICATION

Figures 5b and 6b give a quantitative representation of deposition in fibrous filter media in the absence of significant thermal, electrostatic, or gravitational effects. They are specific however for an interaction number of 1,270 and a density parameter of 89. To obtain a generalization of these curves it would be necessary to obtain similar families of curves for other values of  $N_{sc}$  and  $N_p$ .

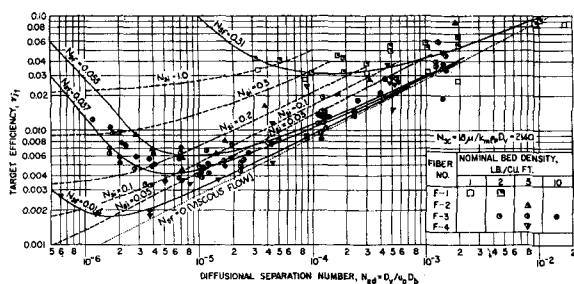
In general lower values of  $N_p$  would be expected to result in higher values of target efficiency. However since  $N_p$  essentially measures residual Reynolds number of flow pattern effects, it is unlikely that variations in this parameter will cause significant deviations from the curves of Figures 5b and 6b,

unless the Reynolds number exceeds 0.1, and will probably not cause major deviations until the Reynolds number exceeds 10.

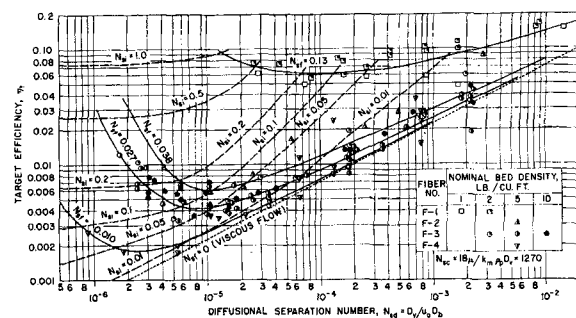
In practice, variations in the value of the interaction number  $N_{sc}$  will be encountered primarily as the result of different aerosol particle sizes. In general for higher values of  $N_{sc}$  curves of constant  $N_{st}$  would be expected to lie below those of Figures 5b and 6b; lower values of  $N_{sc}$  would result in curves above those of Figures 5b and 6b. In either case however curves of constant  $N_{st}$  should approach those of Figures 5b and 6b at high values of  $N_{sc}$  and  $N_{sc}$ , respectively (that is at the right-hand side of each figure). In other words for high values of  $N_{sc}$  and  $N_{sc}$  the curves of Figures 5 and 6 would be sensibly independent of the value of  $N_{sc}$ . This conclusion follows from the fact that  $N_{sc}$  measures the added effect of the deposition mechanism that is not specified in the solid curves of Figures 5b and 6b. Since for either very high values of  $N_{sc}$  or  $N_{sc}$  either inertial or diffusional deposition, respectively, will be controlling, this added effect will be relatively negligible. Similarly at very high values of  $N_{st}$  the effect of variations in  $N_{sc}$  will become minimal.

In the absence of more extensive data defining the complete families of curves for various values of  $N_{sc}$  the following procedure is suggested for utilizing Figures 5b and 6b to obtain a first order design approximation. For the specific values of the separation numbers  $N_{st}$ ,  $N_{sc}$ , and  $N_{sc}$  involved in a particular problem, obtain from Figures 5b and 6b the target efficiency indicated for each of the three combinations of two of these separation numbers. To obtain the target efficiency corresponding to the  $N_{sc}$  and  $N_{sc}$  combination it will be necessary to refer to the long-dashed curves. In general this will yield three values of





a. Uncorrected (based on original data).



b. Corrected (as discussed in Appendix).

Fig. 6. Target efficiency as a function of the diffusional separation number.

target efficiency. For the singular case where  $N_{sc}$  is equal to 1,270 all three values of target efficiency so obtained will, of necessity, come out equal. If the actual value of  $N_{sc}$  involved is less than 1,270, use the highest of these three target-efficiency values; if  $N_{sc}$  is greater than 1,270, use the lowest value of  $\eta_t$ .

In the correlations given here the interaction number has been specified as a parameter. It would be equally rigorous to use the conventional Schmidt number as an alternative. The choice between the two would depend entirely on which proves to be the more convenient or expedient; in other words which one would result in the least spreading of curves of constant  $N_{sc}$  due to variations in the two parameters. This can only be established by additional data in which these two parameters are varied widely.

It will be noted that the term  $k_m$  appears in both  $N_{sc}$  and  $N_d$ . This comes about from the empirical way in which mean free-path effects on aerosol particle motion have been allowed for by the use of the  $k_m$  factor as a correction for viscosity in defining  $N_{sc}$  and  $N_{sd}$ . In the more general case mean free-path effects may also influence the flow around the fiber as discussed by Langmuir (6). This effect can be of practical significance either with fibers much smaller than  $1\text{-}\mu$  diam. or for operation at very low gas pressures, as at high altitude. Such effects would result in higher target efficiencies than would be predicted in their absence. To handle this general case an additional parameter, the Knudsen number, must be introduced (9) into Equations (4). The Knudsen number may be used to measure mean free-path effects both on the aerosol particle and on the collecting fiber by the omission of  $k_m$ ; when one retains the  $k_m$  term as in the present definitions, it may be used to measure only the added influence on flow around the fiber. It is also possible to use the term  $k_m$  as a sole measure of all mean free-path effects, since for specific

values of  $N_{sc}$  and  $k_m$  the Knudsen number is determined. Here again the most expedient approach can only be determined by additional data based on very low pressure filtration tests.

### SUMMARY AND CONCLUSIONS

Data have been obtained on the deposition of aerosols on glass fibers over a wide range of filtration velocities, fiber sizes, and pad densities (Table 2). The data clearly demonstrated the reduction in collection efficiency with increase in velocity at low velocities where diffusion is controlling, the increase in collection efficiency with increase in velocity at high velocities where particle inertia is controlling, and the relative independence of collection efficiency and velocity at intermediate velocity levels where flow-line interception is significant or predominant.

Evaluation of the data in terms of existing theories of deposition, which vary widely amongst themselves, indicated nominal agreement with the theory of Langmuir (6), as modified by Natanson (11), for diffusional deposition.

A method has been presented for generalizing the principles governing deposition of aerosol particles in fibrous packing by the combined effects of flow-line interception, inertial interception, and diffusional deposition. Good correlation of the experimental data was obtained by this method. However a need for specific additional data was indicated to provide ranges necessary for general design utilization. The nature of deviations to be expected for such extended ranges is discussed together with a means for extrapolating the present data to arrive at design approximations in the absence of such additional data.

### ACKNOWLEDGMENT

The assistance rendered by the following is gratefully acknowledged: Owens-Corning Fiberglas Corporation for providing the glass fibers; E. I. duPont de

Nemours and Company, Inc., for providing the dye used for the aerosol; Dr. A. F. Prebus, Ohio State University, for assistance in fiber measurements; the Ohio State University Development Fund for an equipment grant; and Shell Oil Company for a graduate fellowship.

### NOTATION

- $a$  = proportionately constant, dimensionless
- $A_f$  = superficial filter pad area, sq. cm.
- $D_b$  = representative dimension or diameter of collecting body, cm.
- $D_p$  = aerosol particle diameter, cm.
- $D_o$  = diffusion coefficient for aerosol particle =  $k_m RT/3\pi\mu N_A D_p$ , sq. cm./sec.
- $D.F.$  = decontamination factor, =  $\log_{10} [1/(1 - \eta_t)]$
- $e$  = base of natural logarithms, = 2.71828...
- $k_m$  = Stokes-Cunningham correction factor for mean free path of gas molecules, dimensionless
- $k_s$  = sticking factor; fraction of aerosol particles striking fiber surface which remain adhering (reference 8), dimensionless
- $\ln$  = logarithm to base  $e$
- $L_f$  = depth of filter pad, cm.
- $M$  = molecular weight of gas, g./g.-mole
- $m_f$  = mass of filter pad, g.
- $N_A$  = Avogadro's number =  $6.025 \times 10^{23}$  molecules/g.-mole
- $N_{Re}$  = Reynolds number =  $\rho u_0 D_b / \mu$ , dimensionless
- $N_{sc}$  = interaction number =  $18\mu / k_m \rho_p D_o = N_{sf}^2 N_{sd} / N_{sa}$ , dimensionless
- $N_{sd}$  = diffusional separation number =  $D_o / u_0 D_b$ , dimensionless
- $N_{sf}$  = flow-line separation number =  $D_p / D_b$ , dimensionless
- $N_{so}$  = gravitational separation number =  $u_1 / u_0$ , dimensionless
- $N_{si}$  = inertial separation number =

$k_m \rho_p D_p^2 u_o / 18 \mu D_b$ , dimensionless

$N_t$  = number of transfer units, dimensionless

$N_p$  = density parameter =  $k_m \rho_p / 18 \mu = N_{st} / N_{sc} N_{st}^2$ , dimensionless

$R$  = gas constant =  $8.317 \times 10^7$  (erg.)/(g. mole) ( $^{\circ}\text{C}$ .)

$T$  = gas temperature,  $^{\circ}\text{K}$ .

$u_o$  = superficial filter medium velocity (that is velocity based on area  $A_f$ ), cm./sec.

$u_t$  = gravitational terminal settling velocity of aerosol particle, cm./sec.

#### Greek Letters

$\epsilon_p$  = porosity; fractional volume of filter pad not occupied by fiber, dimensionless

$\eta_f$  = pad efficiency; weight fraction of aerosol particles entering pad collected in pad, dimensionless

$\eta_t$  = fiber target efficiency; weight fraction of aerosol particles, in air volume swept out by fibers, that is deposited on fibers, dimensionless

$\mu$  = gas viscosity, poises

$\rho$  = gas density, g./cc.

$\rho_b$  = true density of collecting body fibers, g./cc.

$\rho_p$  = aerosol particle density, g./cc.

$\psi$  = function of

#### LITERATURE CITED

- Blasewitz, A. G., et al., *Document HW-20847*, General Electric Company, Hanford Works (April 16, 1951).
- Chen, C. Y., *Chem. Rev.*, **55**, 595-623 (1955).
- Davies, C. N., *Proc. Inst. Mech. Engrs. (London)*, **1B**, 185-213 (1952); *The Ninth International Congress on Industrial Medicine*, London (Sept. 13-17, 1948).
- La Mer, V. K., et al., *Rept. No. NYO-512*, Contract No. AT-(30-1)-651, Columbia Univ., New York (1951).
- La Mer, V. K., G. Goyer, R. Gruen, and J. Kruger, *Report NYO-514*, Columbia, Univ., New York (June 30, 1952).
- Langmuir, I., *O.S.R.D. Rept. No. 865 (PB 99669)* (Sept. 4, 1942).
- , and K. B. Blodgett, *Rept. No. RL 225*, General Electric Co. (Dec. 1944-July 1945); *Tech. Rept. No. 5418 (PB 27565)*, Army Air Force (Feb. 19, 1946).
- Lewis, W. K., and J. M. Smith, *O.S.R.D. Rept. 1251 (PB 28614)*, (Dec. 15, 1942).
- Lunde, K. E., and C. E. Lapple, *Chem. Eng. Progr.*, **53**, 385-391 (1957).
- Marshall, C. G., Ph.D. thesis, Ohio State Univ., Columbus, (1956).
- Natanson, G. L., *Akad. Nauk SSSR Proceedings*, Section Physical Chem., **112**, 21-25 (1957).
- Ranz, W. E., Univ. of Illinois, Eng. Exp. Sta. *Tech. Rept. No. 3, SO-1004*, Univ. Illinois, Eng. Exp. Sta. (March 31, 1951).
- , and J. B. Wong, *Ind. Eng. Chem.*, **44**, 1371-81 (1952); *Archiv Ind. Hyg. and Occupational Medicine*, **5**, 464-77 (1952); *Univ. of Illinois Eng. Exp. Sta. Tech. Rept. No. 4, SO-1005*, (July 31, 1951).
- Saxton, R. L., and W. E. Ranz, *Tech. Rept. No. 6, SO-1007*, Univ. Ill., Eng. Exp. Sta. (Dec. 31, 1951); *J. Appl. Physics*, **23**, 917-23 (1952).
- Sell, W., *Forsch. Gebiete Ingenieurw.*, **2**, Forschungsheft No. 347 (August, 1931).
- Stairmand, C. J., *Trans. Inst. Chem. Engrs. (London)*, **28**, 130-139 (1950).
- Wright, T. E., R. J. Stasny, and C. E. Lapple, *Rept. 55-457 (AD-142075; PB 131570)*, Donaldson Co., Wright Air Development Center Tech. (Oct. 1957).

Manuscript received July 12, 1960; revision received October 24, 1960; paper accepted October 24, 1960.

#### APPENDIX

In recent investigations subsequent to the above study certain factors were revealed which reflect on the absolute accuracy of the above data, although they do not affect the general validity of the data and correlations. In order to clarify the record it is the purpose of this note to present these subsequent findings and their influence on the above data.

Using essentially the same basic equipment and aerosol used in the above study Marshall (10) found that in order to obtain a correct particle size analysis with a stationary jet impactor it is necessary to restrict the amount of aerosol collected by the impactor slide below a certain critical value (on the order of 0.01 mg. of dye for a jet having a 0.02-cm. slot, 1 cm. long). Greater accumulations of dye indicated progressively larger apparent particle sizes because of interception by previously deposited material. The use of a viscous liquid coating on the impactor slide did not prevent this effect. It is believed that this phenomenon will be encountered with any solid or supercooled-liquid aerosols.

In the above study this effect was not recognized, and jet impactor deposits were heavier than permissible on the basis of Marshall's findings. Thus the true aerosol diameter was probably lower than the value of 0.4  $\mu$  reported. In this more recent study Marshall obtained a mass median diameter of 0.29  $\mu$  for the same dye aerosol, generated at the same operating conditions in substantially the same equipment. Unfortunately however some minor mechanical changes had also been made in the generator. Thus while it cannot be certain that Marshall's aerosol was entirely the same as the one used in the currently reported study, it is believed that this was the case, as adjudged by Marshall's apparent particle-size results when operating the same jet impactors at comparable deposit densities.

In another subsequent and closely related study at another location Wright et al. (17) concluded that the electron micro-

scope technique used for measuring fiber diameter yielded erroneously low average fiber diameters. This was first discovered with Owens-Corning type B glass fiber for which values of specific surface average diameters of 5.60 and 2.85  $\mu$  were obtained with the optical and electron microscopes, respectively. This difference was attributed to a selective fracturing of the finer fibers in mounting techniques used for preparing the electron microscope slides; no fracturing was involved with the optical microscope. A similar check on a type AA glass fiber gave specific surface average diameters of 3.3 and 1.86  $\mu$  with the optical and electron microscopes, respectively. In the currently reported study fiber F-1 was a type AA fiber and was measured with the identical electron microscope mounting technique. It is believed therefore that the true average fiber diameter should be larger than the 1.29  $\mu$  reported. Although fiber F-1 was from an entirely different lot than Wright's type AA fiber, the ratio of diameters obtained by Wright with the two techniques should be applicable to obtain an approximation of the corrected diameter of fiber F-1. On this basis a corrected value of 2.3  $\mu$  is obtained for the specific surface average diameter of fiber F-1. A correction of this type is not involved in the case of fibers F-2, F-3, and F-4, all of which were relatively uniform fibers measured with the optical microscope.

When one applies the corrections indicated by the more recent findings of both Marshall (10) and Wright (17), the following corrections to the original data reported in the current paper would be indicated:

#### Corrected aerosol properties:

	Original value	Corrected value
$\rho$ , g./cc.	$1.25 \times 10^{-3}$	$1.25 \times 10^{-3}$
$\rho_p$ , g./cc.	1.26	1.26
$\mu$ , centipoises	0.0183	0.0183
$D_p$ , $\mu$	0.40	0.29
$k_m$	1.42	1.59
$D_v$ , sq. cm./sec.	$8.6 \times 10^{-7}$	$1.30 \times 10^{-6}$
$u_t$ , cm./sec.	$8.5 \times 10^{-4}$	$5.0 \times 10^{-4}$
$N_{sc}$	2,140	1,270
$N_p$	80	89

#### Corrected values of correlation parameters:

Parameter correction factor (Value by which original parameter must be multiplied to obtain corrected parameter)				
Fiber number	$\eta_t$	$N_{st}$	$N_{sc}$	$N_{sd}$
F-1	1.78	0.41	0.33	0.85
F-2	1.00	0.73	0.59	1.51
F-3	1.00	0.73	0.59	1.51
F-4	1.00	0.73	0.59	1.51

The above factors give the magnitude of the correction inferred from these later works. The correlations based on the original data are shown in Figures 5a and 6a. Figures 5b and 6b were derived from Figures 5a and 6a by applying the above correction factors to the individual data points.